Article:
Milanesi, L., Waltho, J.P., Hunter, C.A. et al. (2012) Measurement of energy landscape roughness of folded and unfolded proteins. Proceedings of the National Academy of Sciences, 109 (48). pp. 19563-19568. ISSN: 0027-8424

https://doi.org/10.1073/pnas.1211764109

Measurement of Energy Landscape Roughness of Folded and Unfolded Proteins

Lilia Milanesi[a,b,1], Jonathan P. Waltho[a,c], Christopher A. Hunter[b], Daniel J. Shaw[d,2], Godfrey S. Beddard[d], Gavin D. Reid[d], Sagarika Dev[e,3], and Martin Volk[e,4]

[a]Department of Molecular Biology and Biotechnology, University of Sheffield, Sheffield S10 2TN, UK;

[b]Department of Chemistry, University of Sheffield, Sheffield S10 2TN, UK;

[c]Manchester Interdisciplinary Biocentre, 131 Princess St., Manchester. M1 7DN, UK;

[d]School of Chemistry, University of Leeds, Leeds LS2 9JT, UK;

[e]Department of Chemistry, University of Liverpool, Liverpool L69 3BX, UK.

[1]Present address: Department of Neurodegenerative Disease, UCL Institute of Neurology, London WC1N 3BG, UK.

[2]Present address: Department of Physics, University of Strathclyde, Glasgow G4 0NG, UK.

[3]Present address: Department of Chemistry, MCM DAV College for Women, Chandigarh, India.

[4]To whom correspondence should be addressed: m.volk@liv.ac.uk

Classification: PHYSICAL SCIENCES – Chemistry;
BIOLOGICAL SCIENCES – Biophysics.

Corresponding author: Dr. Martin Volk
Department of Chemistry
University of Liverpool
Liverpool L69 3BX, UK
Tel. +44-151-794-3317
m.volk@liv.ac.uk

Abstract

The dynamics of protein conformational changes, from protein folding to smaller changes, such as those involved in ligand binding, are governed by the properties of the conformational energy landscape. Different techniques have been employed to follow the motion of a protein over this landscape and thus quantify its properties. However, these techniques are often limited to short time scales and low energy conformations. Here we describe a general approach that overcomes these limitations: Starting from a non-native conformation held by an aromatic disulfide bond, we use time-resolved spectroscopy to observe non-equilibrium backbone dynamics over nine orders of magnitude in time, from picoseconds to milliseconds, after photolysis of the disulfide bond. We find that the re-encounter probability of residues that are initially in close contact decreases with time following an unusual power law that persists over the full time range and is independent of the primary sequence. Model simulations show that this power law arises from subdiffusional motion, indicating a wide distribution of trapping times in local minima of the energy landscape, and enable us to quantify the roughness of the energy landscape (4-5 k_BT). Surprisingly, even under denaturing conditions the energy landscape remains highly rugged with deep traps (>20 k_BT) which result from multiple non-native interactions and are sufficient for trapping on the millisecond time scale. Finally, we suggest that the subdiffusional motion of the protein backbone found here may promote rapid folding of proteins with low contact order by enhancing contact formation between nearby residues.

\body

Major advances have been made in recent years in understanding dynamic aspects of protein conformational changes and in particular protein folding. However, many issues still remain to be solved (1). Among these are the properties of the unfolded protein ensemble and the role of residual structure of denatured proteins in promoting folding (2), the heterogeneity of microscopic folding pathways (3) and the existence of multiple distinct, but only transiently populated, intermediates (4). Particularly for fast folding proteins, the idea of downhill folding, i.e. the absence of a significant barrier, has been suggested as an alternative mechanism (5, 6), but it is not clear to what extent fast folding proteins make use of this mechanism. On the other hand, technical progress has made it possible to observe multiple folding and unfolding events in millisecond all-atom molecular dynamics simulations. Such simulations have shown that some proteins always follow the same folding pathway, whereas others have several different pathways (7). Moreover, individual folding events occur with sub-microsecond transit times through a distinct transition state, but are separated by long waiting times, which yield the experimentally observed folding times (8).

The idea of motion on a rugged energy landscape (9-11) has been used widely to describe conformational changes in proteins, including protein folding. As a result of the multitude and varying strength of local and non-local interactions of the polypeptide backbone, side chains and solvent molecules, the multidimensional conformational energy landscape is thought to consist of a hierarchy of local minima of varying depths (Fig. 1). The properties of this energy landscape govern the motion of the polypeptide backbone in real space, and thus a full understanding of processes

like protein folding or ligand binding will require a better characterisation of this landscape. In practise, motion on the multi-dimensional energy landscape must be approximated by diffusion on an idealised low-dimensional surface, the speed of which is limited by solvent viscosity and internal friction arising from the roughness of the full energy landscape (12). It is noteworthy that energy landscape roughness has been implicated directly in causing non-exponential folding kinetics (5, 6). Similarly, the experimentally observed increase of the transition state transit time at higher temperatures was explained by stronger internal friction due to increased energy landscape roughness (13, 14).

Some progress has been made in experimentally observing motion over the energy landscape on short time scales. In particular, intra-peptide contact formation has been investigated extensively using fluorescence and triplet quenching (15-19). These experiments observe intra-chain loop formation from an equilibrium distribution of initial conformations and provide important information on polypeptide backbone diffusion, including the effects of excluded volume and chain stiffness. Non-exponential dynamics were observed on the picosecond time scale and were assigned to motion of the polypeptide backbone within a local basin of the energy landscape (17). Diffusion of the polypeptide over larger distances in conformational space involves transitions over higher energy barriers separating the local basins and has been observed on the nano- to microsecond time scale. Structural changes corresponding to transitions over even larger barriers, e.g. due to formation of secondary and tertiary structure, should occur on longer time scales but are not accessible with methods whose time scale is limited by the intrinsic lifetime of the reporter state (18). More recently, single-molecule fluorescence correlation

spectroscopy was used which in principle extends the time window to milliseconds, but is affected by triplet blinking on the microsecond time scale (20). Similarly, ligand binding experiments extend the time window to milliseconds, but are limited to specific proteins (21).

An alternative approach for the observation of backbone dynamics is described here; this uses geminate recombination of a photo-cleaved aromatic disulfide bond which initially holds the protein in a non-native conformation (Fig. 2) (22, 23). This method observes the opposite of loop formation, namely the separation of two residues which initially are in close contact. As the residues separate due to polypeptide backbone motion, their encounter probability decreases, which leads to a decreasing rate of geminate recombination. Thus, the decay of the transient thiyl radical concentration, which is readily measured using the strong absorbance of aromatic thiyl radicals near 500 nm (22), can be used to monitor the dynamics of the polypeptide backbone. Whereas quenching experiments observe loop formation from an equilibrium distribution of conformations, which excludes all conformations that lie higher than a few $k_B T$, where k_B is the Boltzmann constant and T the temperature, on the potential energy landscape, disulfide recombination monitors processes far from equilibrium, providing complementary information, with, importantly, no intrinsic time limit.

The disulfide recombination method requires an aromatic disulfide bond because non-aromatic thiyl radicals do not recombine fast enough to report on backbone dynamics (24). This approach has consequently been used only for short peptides (22, 23) which can be synthesized using solid-phase techniques. Although advances in non-natural amino acid mutagenesis and chemical ligation methods allow the functionalisation of

proteins with photosensitive moieties, examples of intramolecular photosensitive cross-linkers still are rare. We recently introduced an aromatic disulfide cross-link into a 174 amino acid protein (the N-terminal domain of phosphorglycerate kinase from *Geobacillus steareothermophylus*, N-PGK) (25). At low denaturant concentrations (0-2 M urea), the cross-linked protein has a molten-globule like conformation with reduced tertiary structure and reduced stability, see Appendix II (Supplementary Information). When the disulfide cross-link is cleaved by addition of a reducing agent, the protein folds into the native structure (25). Thus, photolysis of the disulfide bond at low urea concentrations is expected to trigger structural changes of the protein from the partially unfolded towards the folded structure (Figure 2). At 8 M urea, both the cross-linked and the open protein are denatured, but photolysis of the disulfide bond will still alter the range of conformations that are accessible at equilibrium (25). Here, we report the recombination dynamics of the thiyl radicals after photolysis of cross-linked N-PGK, both for low and high concentrations of urea, and show that their re-encounter probability decreases with time following a universal power law over nine orders of magnitude in time, from picoseconds to milliseconds, regardless of primary sequence or the presence of secondary or tertiary structure. Model simulations show that this power law arises from subdiffusional motion of the residues, indicating a wide distribution of trapping times in local minima of the energy landscape and enabling us to quantify the energy landscape roughness. Furthermore, we suggest that the subdiffusional motion of the protein backbone is a likely candidate for promoting rapid folding, particularly of proteins with low contact order, by enhancing contact formation between nearby residues.

Results

Thiyl Radical Recombination Dynamics. The transient absorbance near 500 nm, which is a direct measure of thiyl radical concentration (22), was recorded from 1 ps to 1 ms after UV-photolysis of cross-linked N-PGK (Figure 3). The fast appearance of the absorbance, Figure 3A, confirms aromatic disulfide bond splitting within 1.5 ps after absorption of a UV photon, as found in model aromatic disulfides (22, 26). The decay of this transient absorbance shows that, initially, geminate recombination is very fast due to the radicals being generated in close proximity. As the protein relaxes towards its new equilibrium conformation, the radicals are separated to increasingly larger average distances. On longer time scales and for low concentrations of urea, the radicals may be further held apart by the formation of secondary and tertiary structure. Both effects lead to a decrease of the probability of a re-encounter, and hence to a slowing of the recombination of the surviving thiyl radicals. As a consequence, thiyl radical recombination spans many orders of magnitude in time. Figure 4 shows that the instantaneous rate constant for recombination, $k_{inst}(t) = -(dc(t)/dt)/c(t)$, where t is the time after photolysis and $c(t)$ is the surviving radical concentration, follows a highly unusual power law, $k_{inst}(t) \sim t^{-0.94(\pm 0.03)}$, over the full experimental time window. Most intriguingly, the same power law is found in the absence of significant secondary or tertiary structure (8 M urea) as under conditions of persistent native-like secondary structure (0-2 M urea). Although the timescales that were investigated are shorter (ps to few μs), the same power law had also been found for synthetic α-helical peptides (Figure 4) (22). Our results on N-PGK now show that the $k_{inst}(t) \sim t^{-0.94}$ power law is an intrinsic property of the polypeptide backbone and does not depend on details of sequence or secondary and tertiary structure.

Simulation of Residue Encounter Probability. To identify the origin of this dynamic behavior we undertook a series of numerical simulations, incorporating various aspects of polypeptide dynamics. These simulations calculate the time-dependent survival probability, $P(t)$, of two radicals which initially are in close contact and undergo diffusion-controlled geminate recombination. From $P(t)$, the instantaneous rate constant $k_{inst}(t) = -(dP(t)/dt)/P(t)$ can be calculated and compared to the experimental results. Full details of the simulations and their results are given in Appendix III (Supplementary Information).

For normal diffusion of the contact forming residues, the mean square displacement of a residue undergoing random walk increases linearly with time, $\langle r^2(t) \rangle \propto t$. For untethered radical pairs undergoing normal diffusion, the solution for the time-dependent survival probability during geminate recombination can be expressed in analytical closed form (29), which agrees well with experimental results for aromatic thiyl radicals (30). This survival probability yields an initial power law for the instantaneous rate constant $k_{inst}(t) \sim t^{-0.5}$, turning into $k_{inst}(t) \sim t^{-1.5}$ once diffusion has taken place over a length scale comparable to the radical pair contact distance. With typical values for backbone diffusion coefficients from quenching experiments (15-18) and aromatic thiyl contact distances from experiments on model compounds (30), this transition is estimated to occur on the ns-time scale, see Figure S3 (Supporting Information). However, this neglects the tethering effect of the polypeptide chain which links the two radicals. Following the standard approach for this problem, the tether was approximated by assuming the radicals to be subject to normal diffusion, albeit under the constraints of a harmonic potential. Numerical simulations of the survival probability of geminately recombining radicals under this constraint show the

same initial behavior as for freely diffusing radicals, with a transition from $k_{inst}(t) \sim t^{-0.5}$ to $k_{inst}(t) \sim t^{-1.5}$ on the ns-time scale, see Appendix III (Supporting Information). This is followed by conformational equilibration in the harmonic potential, corresponding to diffusion over the length scale of the tether, within approx. 1 μs, when $k_{inst}(t)$ becomes time-independent, see Figure S5 (Supporting Information).

Other important aspects of the dynamic behavior of the polypeptide backbone are chain stiffness and excluded volume effects. These effects tend to disfavor conformations with short radical-radical separation, particularly if the radicals are separated by only relatively short backbone sections, and thus could be expected to lead to faster initial separation of the radicals. We accounted for these effects by numerically simulating radical diffusion and recombination in various modified potentials which were derived from theoretical models, simulations or experimental results for the equilibrium end-to-end distance distribution of short peptide sections. Full details and mathematical expressions of these potentials, as well as the results of our simulations, are given in Appendix III (Supporting Information). All of these simulations yielded only minor modifications of the general recombination behavior in a harmonic potential, see Figs. S6-S10 (Supporting Information), and thus failed to reproduce the experimental behavior of $k_{inst}(t)$. Therefore, the observation that $k_{inst}(t) \sim t^{-0.94}$ over the full time range from picoseconds to milliseconds is not consistent with normal diffusion of the peptide sections to which the radicals are bound, even when accounting for tethering, chain stiffness and excluded volume effects.

On the other hand, simulations where the peptide residues are assumed to follow "subdiffusional" behavior successfully account for the unusual power law,

$k_{inst}(t) \sim t^{-0.94}$. Subdiffusion means that the mean square displacement of a particle (in the absence of a constraining potential) is nonlinear in time, $\langle r^2(t) \rangle \propto t^{\alpha}$ with $\alpha < 1$, and implies quasi-random motion with a wide distribution of trapping times (30). Our subdiffusion simulations are based on the approach by Seki *et al.* (31), which models geminate recombination for untethered particles that undergo random jumps in three-dimensional space with a broad distribution of waiting times before the next jump, resulting from an exponential distribution, $g(E)$, of the jump activation energy, E, Fig. 1B; mathematical details are given in Appendix III (Supporting Information). Figure 5A shows typical results for the time dependent instantaneous rate constant, $k_{inst}(t)$, obtained from these simulations for different values of the subdiffusional parameter α. As expected, for $\alpha = 1$ this model yields the same result as found from the simulations which assume normal diffusion, i.e. an initial power law for the instantaneous rate constant $k_{inst}(t) \sim t^{-0.5}$ which turns into $k_{inst}(t) \sim t^{-1.5}$ at later times, with the transition determined by the radical pair contact distance. Upon decreasing α, i.e. for increasingly subdiffusional behavior, the power of $k_{inst}(t)$ for the initial phase increases, whereas that for the later phase decreases (Figure 5B). When α is around 0.3, the two phases of $k_{inst}(t)$ merge into a single power law, $k_{inst}(t) \propto t^{-0.95}$. This time dependence holds over at least nine orders of magnitude in time in our simulations and closely resembles the experimental observation, Figure 4; the results do not significantly depend on the other model parameters used in the simulations, see Figure S11 (Supporting Information). We conclude that the experimentally observed $k_{inst}(t) \sim t^{-0.94}$ power law is the result of subdiffusional motion of the residues holding the thiyl radicals after disulphide bond photolysis.

These simulations ignore the tethering effect of the polypeptide backbone. As in the case of normal diffusion, it is expected that the radicals eventually reach an equilibrium distribution and that the instantaneous rate constant for recombination, $k_{inst}(t)$, then does not change any further with time. In principle, this could be simulated by assuming subdiffusive motion in a harmonic potential, which can be described by the fractional Fokker-Planck equation (33), although this is beyond the scope of the current paper. However, it has been shown that the approach to equilibrium for this situation is significantly slower than in the case of normal diffusion (33); it is reasonable to assume that this slower equilibration in the case of subdiffusion contributes to the fact that no leveling off of $k_{inst}(t)$ is observed in our experimental data even at the longest time scale (1 ms).

Discussion

Roughness of the Protein Energy Landscape. Our results show that the polypeptide backbone in proteins is not subject to normal diffusional behavior. Instead, a subdiffusional model is required to account for the experimental observations. Subdiffusional behavior of certain aspects of polypeptide backbone dynamics has been reported on the pico- to nanosecond time scale from neutron scattering experiments (34) and molecular dynamics simulations (35) and on the millisecond to second time scale from single molecule electron transfer measurements (36). However, these results refer to small-scale equilibrium fluctuations, and it is not clear to what extent their conclusions can be extrapolated to large-scale non-equilibrium conformational changes. Our experimental results were obtained under non-equilibrium conditions, and thus show that intra-protein subdiffusion not only occurs

during small-scale equilibrium fluctuations, but also governs large-scale motions, such as those taking place during protein folding.

In general, subdiffusional behavior arises from the random motion of diffusing particles which encounter local traps with a wide distribution of trapping times (31). In the context of intra-protein residue subdiffusion, the distribution of trapping times are due to a wide range of barrier heights (or depths of local minima) present on the conformational energy landscape (37) (Figure 1); as the polypeptide backbone relaxes towards the new equilibrium distribution following photolyis of the disulfide bond, some proteins become trapped in local minima which hold the radicals apart, thus preventing their rapid recombination. Thus, our results yield confirmation of the existence and relevance of a wide range of barrier heights, due to a rugged potential energy landscape, even during large-scale protein conformational changes. Furthermore, the observation that good agreement between the simulated time dependence of $k_{inst}(t)$ and the experimentally observed power law, $k_{inst}(t) \propto t^{-0.94}$, is found for a value of α near ~ 0.3 (Figure 5) allows us to estimate the width of the barrier height distribution and thus the roughness of the potential energy landscape. Assuming an exponential distribution of the jump activation barriers, $g(E) \sim \exp(-\alpha E/k_B T)$, as used in the model by Seki *et al.* (32), a value of α near ~ 0.3 corresponds to an average barrier height $\langle E \rangle \sim 3\text{-}4\ k_B T$, and a root-mean-squared roughness, $\varepsilon = \langle E^2 \rangle^{1/2}$, which is the parameter normally used to quantify roughness, of ~ 4-5 $k_B T$.

Potential transient interactions that would result in local minima of the energy landscape are hydrogen bonding, electrostatic interactions between ionized or polar

residues and hydrophobic interactions between nonpolar residues, including van-der-Waals forces and π-π aromatic interactions. Protein engineering experiments indicate that a single hydrophobic side chain contact, such as a Phe-Phe aromatic interaction, contributes about 5 kJ/mol (2 k_BT) to the stability of a folded protein (38); a single hydrogen bond contributes about 2-7 kJ/mol (~ 1-3 k_BT) (39), and a surface exposed salt bridge contributes about 2 kJ/mol (~ k_BT) (40). These values are of the same order of magnitude as the landscape roughness determined from our experimental results, which suggests that many local minima may arise from a single interaction. However, because a broad distribution of trapping energies is required to account for subdiffusional behavior, a significant fraction of the minima is deeper than 2 k_BT, and thus must be due to the combined effect of two or more such interactions.

The roughness of the folding energy landscape found here is somewhat smaller than the roughness of protein-ligand interaction landscapes (5-8 k_BT) of bimolecular protein complexes (41) and similar to the roughness of bacteriorhodopsin (4-6 k_BT) (42) which were suggested by the temperature dependence of single molecule dynamic force spectroscopy data. Similar results on filamin could be interpreted as arising from a landscape roughness of 4 k_BT, although a completely different interpretation of the experimental observations is preferred by the authors (43), raising some uncertainty over the interpretation of such force-stretching experiments. Roughness values of 1.3-2.6 k_BT were suggested for the folding energy landscape from slow backbone diffusion observed in unfolded proteins (27, 28), but these values are based on problematic estimates of the speed of diffusion of the backbone in the absence of roughness. From similar observations, a roughness of 1.7 k_BT was suggested for unstructured oligopeptides (15), which may reflect weak residue-residue

interactions in such peptides. It must be noted that all of these estimates of energy landscape roughness are based on the theory of diffusion in a one-dimensional rough potential (44), which normally is assumed to be the projection of the multidimensional potential onto the reaction coordinate. However, motion of a protein does take place on a multidimensional landscape, which modifies the diffusion behavior; for example, high barriers can be circumvented, which is not possible in a one-dimensional potential, and it is not clear to what extent the use of the one-dimensional diffusion theoretical treatment may distort these results. In contrast, the roughness parameter determined here directly refers to the local variation of the potential energy of the multidimensional energy landscape; in any case, this may not be the same as the roughness of the idealised reaction potential, which effectively averages over many conformations and microscopic reaction pathways.

Deep Traps on the Protein Energy Landscape. Subdiffusion arising from a wide range of trapping times should persist only up to time scales corresponding to the longest trapping times (31) and normal diffusional behavior should be found at longer times. Our experiments show that in N-PGK these trapping times extend across the entire timescale from picoseconds to milliseconds. A trapping time of 1 ms suggests a barrier of the order of 50 kJ/mol (20 k_BT), assuming a typical value for the pre-exponential factor in the range $10^{11} – 10^{13}$ s^{-1}. As detailed above, individual residue-residue interaction energies have values of the order 5 kJ/mol. This indicates that, although the average barrier height is of the order 3-4 k_BT, proteins temporarily adopt conformations that are stabilized by multiple interactions, leading to very deep minima on the rugged energy landscape. The range of long trapping times observed in

these experiments therefore implies that the protein samples a diverse ensemble of states that contain multiple native or non-native interactions, or a combination thereof.

Conformational dynamics on the millisecond timescale are also accessible from NMR measurements. Under denaturant conditions comparable to our 2 M urea experiments, a collapsed, compact state of N-PGK with some non-native secondary structure and many non-native tertiary contacts rapidly forms and is substantially populated prior to folding to the native state (45). Population of this molten globule state leads to NMR-line broadening, which indicates that the component species have trapping times on the millisecond time scale (46). Indeed, the NMR line-broadening (47) and complex interconversion behavior over a wide range of time scales (48) that are typical features of molten globule states are readily accounted for by subdiffusional behavior on a rugged energy landscape as proposed here.

Significantly, we also observe subdiffusional behavior with trapping times up to milliseconds in N-PGK at denaturant concentrations where the protein does not fold and where population of the collapsed state is no longer detectable by NMR (8 M urea). This indicates that even under denaturing conditions the energy landscape of real proteins remains rugged, to the extent of providing energy minima with trapping times on the millisecond time scale (i.e. having a depth of ~20 k_BT). Our observations substantially extend the time scale of the relevance of hierarchical energy landscapes in denatured or unfolded proteins. Previously, these had been observed only for short oligopeptides (17), where they are limited to the sub-nanosecond time scale and full conformational equilibration is achieved on the 10 ns – 1 μs time scale (15-17) due to peptide design which excluded strong residue-residue interactions. Close inspection of

triplet quenching experiments on denatured proteins show slight indications of non-exponential dynamics on the 10-100 us time scale that might indicate deeper traps (18). The existence of significant interactions in unfolded proteins had been suggested previously on the basis of photochemically induced dynamic nuclear polarization NOE (49) and paramagnetic relaxation enhancement (50) NMR experiments and from the low value and unusual denaturant dependence of their intrapolymer diffusion constant (18). Similarly, the radius of gyration of the unfolded state of different variants of staphylococcal nuclease indicated the formation of transient hydrophobic clusters (51). Our results now confirm that even under conditions where they are assumed to be fully unfolded, proteins indeed become trapped in a wide range of states, some of which are long-lived and stabilized by multiple (primarily non-native) interactions.

Relevance for Protein Folding. In general, the roughness of the energy landscape determines the speed with which the protein moves over this landscape and therefore is relevant for the dynamics of large-scale structural changes, such as those occurring during protein folding, as well as the rate of small-scale conversion between different conformations at or near equilibrium, such as those required for ligand binding. Quantitative information on this parameter so far has been rare. Here we report experimental results indicating significant overall roughness (~4-5 k_BT) as well as the existence of deep traps (>20 k_BT), even in denatured proteins, most likely from multiple non-native interactions; this energy roughness results in strongly subdiffusional behavior of the polypeptide backbone, i.e. the mean square displacement of a polypeptide segment is nonlinear in time, $\langle r^2(t) \rangle \propto t^{\alpha}$ with $\alpha << 1$. Any theoretical treatment of internal polypeptide motion must account for this

behaviour. In particular, this may have important consequences for the theoretical treatment of one-dimensional diffusion along the (folding) reaction coordinate, e.g. for estimating reaction rates using Kramers' theory (12) or simulating diffusion in idealised potentials (8, 13). Currently, such simulations include the roughness of the multidimensional energy surface by assuming an effective friction coefficient; an investigation of the extent to which subdiffusional behavior (in three-dimensional real space) does affect the validity of this approach is beyond the scope of the current paper.

The role of transient non-native interactions in unfolded proteins for the speed of folding has been discussed previously. For example, the transient formation of non-native contacts may bring backbone sections closer together which are far from each other in the primary sequence but close in the native structure, thus accelerating their folding. Such interactions are thought to be responsible for "abnormal" Φ-values (52). More specifically, lattice model simulations directly suggested that they could significantly enhance the rate of folding (52). Folding kinetics experiments using mutations of surface hydrophobic residues are in agreement with this proposal (53). Our observation of the existence of such interactions even in denatured proteins yields further support for this suggestion.

It is even more intriguing to speculate about the role which intra-protein subdiffusion may play in promoting fast folding, especially of proteins with low contact order, i.e. proteins where many native interactions are formed by residues which are close in the primary sequence. Compared to normal diffusion, subdiffusion *enhances* the probability of encountering a *nearby* interaction partner within a given time (54).

Thus, protein structures with low contact order are even more likely to rapidly form their native interactions if the residues undergo subdiffusional motion than if they followed normal diffusion. Subdiffusion of the polypeptide backbone as a result of the highly rugged landscape, therefore, may be an important contributing factor for the observed correlation between the folding times of small proteins and their contact order (55).

Concluding Remarks. We have presented a novel approach for characterizing the properties of the potential energy landscape of proteins. Geminate recombination following photolysis of an aromatic disulfide bond provides evidence for subdiffusional behavior of the polypeptide backbone, with the mean square displacement of a residue showing sub-linear time dependence, $\langle r^2(t) \rangle \propto t^{\alpha}$, with $\alpha \sim 0.3$, over nine orders of magnitude in time from picoseconds to milliseconds. This observation shows the existence of a wide range of trapping times and provides a measure of the roughness of the potential energy landscape which was found to be of the order 4-5 $k_B T$. However, there are potential energy minima in proteins, stabilized by multiple interactions, which are far deeper than this and extend at least up to 20 $k_B T$. Most intriguingly, both of these results also were observed under denaturing conditions.

Materials and Methods

Disulfide cross-linked N-PGK in 50 mM sodium phosphate buffer, pD 6.6-7, 100 mM NaCl was prepared as described in reference (25) and urea added as indicated. Fig. S1 in the Supplementary Information shows that the addition of 2 M urea has no effect on the secondary structural content of the open form of N-PGK, and only a small

effect on the secondary structural content of the cross-linked form. For measurements on the picosecond time scale, disulfide photolysis was achieved with 100 fs laser pulses at 275 nm and absorbance changes were probed using optically delayed 100 fs laser pulses at 560 nm. Measurements on slower time scales used 5 ns laser pulses at 266 nm for disulfide photolysis; continuous light and a fast detector were used for probing absorbance changes. Sample concentration and excitation energy were lower for measurements on the picosecond time scale than for those on the nano- to millisecond time scale, resulting in lower absorbance changes. For all measurements, samples were continuously flowed or rotated to avoid photodamage; no signal degradation was observed during the course of the measurements. Dynamics of the transient absorbance changes within the first few picoseconds may be affected by dielectric and vibrational relaxation (22, 27) and were excluded from further analysis. See Appendix I (Supplementary Information) for full experimental details.

Acknowledgments

The authors would like to thank Dr. Julia Weinstein, University of Sheffield, for the loan of an Ar-ion laser. Financial support from the BBSRC is gratefully acknowledged.

References

1. Sosnick TR, Barrick D (2011) The folding of single domain proteins - have we reached a consensus? *Curr. Opin. Struct. Biol.* 21**:** 12-24.
2. McCarney ER, Kohn JE, Plaxco KW (2005) Is there or isn't there? The case for (and against) residual structure in chemically denatured proteins. *Critical Reviews in Biochemistry and Molecular Biology* 40**:** 181-189.

3. Krishna MMG, Englander SW (2007) A unified mechanism for protein folding: Predetermined pathways with optional errors. *Protein Sci.* 16**:** 449-464.

4. Brockwell DJ, Radford SE (2007) Intermediates: ubiquitous species on folding energy landscapes? *Curr. Opin. Struct. Biol.* 17**:** 30-37.

5. Sabelko J, Ervin J, Gruebele M (1999) Observation of strange kinetics in protein folding. *Proc. Natl. Acad. Sci. USA* 96**:** 6031-6036.

6. Eaton WA (1999) Searching for ‘‘downhill scenarios’’ in protein folding. *Proc. Natl. Acad. Sci. USA* 96**:** 5897-5899.

7. Lindorff-Larsen K, Piana S, Dror RO, Shaw DE (2011) How Fast-Folding Proteins Fold. *Science* 334**:** 517-520.

8. Shaw DE et al. (2010) Atomic-Level Characterization of the Structural Dynamics of Proteins. *Science* 330**:** 341-346.

9. Ansari A et al. (1985) Protein states and proteinquakes. *Proc. Natl. Acad. Sci. USA* 82**:** 5000-5004.

10. Frauenfelder H, Sligar SG, Wolynes PG (1991) The energy landscapes and motions of proteins. *Science* 254**:** 1598-1603.

11. Onuchic JN, Wolynes PG (2004) Theory of protein folding. *Curr. Opin. Struct. Biol.* 14**:** 70-75.

12. Hagen SJ (2010) Solvent viscosity and friction in protein folding dynamics. *Current Protein and Peptide Science* 11**:** 385-395.

13. Liu F, Nakaema M, Gruebele M (2009) The transition state transit time of WW domain folding is controlled by energy landscape roughness. *J. Chem. Phys.* 131.

14. Cellmer T, Henry ER, Hofrichter J, Eaton WA (2008) Measuring internal friction of an ultrafast-folding protein. *Proc. Natl. Acad. Sci. U. S. A.* 105**:** 18320-18325.

15. Lapidus LJ, Eaton WA, Hofrichter J (2000) Measuring the rate of intramolecular contact formation in polypeptides. *Proc. Natl. Acad. Sci. USA* 97**:** 7220-7225.

16. Möglich A, Krieger F, Kiefhaber T (2005) Molecular basis for the effect of urea and guanidinium chloride on the dynamics of unfolded polypeptide chains. *J. Mol. Biol.* 345**:** 153-162.

17. Fierz B et al. (2007) Loop formation in unfolded polypeptide chains on the picoseconds to microseconds time scale. *Proc. Natl. Acad. Sci. USA* 104**:** 2163-2168.

18. Singh VR, Kopka M, Chen Y, Wedemeyer WJ, Lapidus LJ (2007) Dynamic similarity of the unfolded states of proteins L and G. *Biochemistry* 46**:** 10046-10054.

19. Soranno A, Longhi R, Bellini T, Buscaglia M (2009) Kinetics of contact formation and end-to-end distance distributions of swollen disordered peptides. *Biophys. J.* 96**:** 1515-1528.

20. Nettels D, Hoffmann A, Schuler B (2008) Unfolded protein and peptide dynamics investigated with single-molecule FRET and correlation spectroscopy from picoseconds to seconds. *J. Phys. Chem. B* 112**:** 6137-6146.

21. Hagen SJ, Carswell CW, Sjolander EM (2001) Rate of intrachain contact formation in an unfolded protein: Temperature and denaturant effects. *J. Mol. Biol.* 305**:** 1161-1171.

22. Volk M et al. (1997) Peptide conformational dynamics and vibrational Stark effects following photoinitiated disulfide cleavage. *J. Phys. Chem. B* 101**:** 8607-8616.

23. Volk M (2001) Fast initiation of peptide and protein folding processes. *Eur. J. Org. Chem.***:** 2605-2621.

24. Kolano C, Helbing J, Bucher G, Sander W, Hamm P (2007) Intramolecular disulfide bridges as a phototrigger to monitor the dynamics of small cyclic peptides. *J. Phys. Chem. B* 111**:** 11297-11302.

25. Milanesi L et al. (2008) A method for the reversible trapping of proteins in non-native conformations. *Biochemistry* 47**:** 13620-13634..

26. Ernsting NP (1990) Solvation of photolytically generated p-aminophenylthiyl radicals studied by sub-picosecond transient absorption. *Chem. Phys. Lett.* 166**:** 221-226.

27 Nettels D, Gopich IV, Hoffmann A, Schuler B (2007) Ultrafast dynamics of protein collapse from single-molecule photon statistics. *Proc. Natl. Acad. Sci. USA* 104**:** 2655-2660.

28 Waldauer SA, Bakajin O, Lapidus LJ (2010) Extremely slow intramolecular diffusion in unfolded protein L. *Proc. Natl. Acad. Sci. U. S. A.* 107**:** 13713-13717

29. Shin KJ, Kapral R (1978) Kinetic theory of reactive pair dynamics in liquids. *J. Chem. Phys.* 69**:** 3685-3696.

30. Scott TW, Liu SN (1989) Picosecond geminate recombination of phenylthiyl free-radical pairs. *J. Phys. Chem.* 93**:** 1393-1396.

31. Metzler R, Klafter J (2004) The restaurant at the end of the random walk: recent developments in the description of anomalous transport by fractional dynamics. *J. Phys. A-Math. Gen.* 37**:** R161-R208.

32. Seki K, Wojcik M, Tachiya M (2003) Recombination kinetics in subdiffusive media. *J. Chem. Phys.* 119**:** 7525-7533.

33. Metzler R, Klafter J (2000) The random walk's guide to anomalous diffusion: A fractional dynamics approach. *Phys. Rep.* 339**:** 1-77.

34. Paciaroni A et al. (2009) Coupled relaxations at the protein-water interface in the picosecond time scale. *J. Roy. Soc. Interface* 6**:** S635-S640.

35. Senet P, Maisuradze GG, Foulie C, Delarue P, Scheraga HA (2008) How main-chains of proteins explore the free-energy landscape in native states. *Proc. Natl. Acad. Sci. USA* 105**:** 19708-19713.

36. Yang H et al. (2003) Protein conformational dynamics probed by single-molecule electron transfer. *Science* 302**:** 262-266.

37. Luo G, Andricioaei I, Xie XS, Karplus M (2006) Dynamic distance disorder in proteins is caused by trapping. *J. Phys. Chem. B* 110**:** 9363-9367.

38. Serrano L, Bycroft M, Fersht AR (1991) Aromatic-aromatic Interactions and protein stability. Investigation by double-mutant cycles. *J. Mol. Biol.* 218**:** 465-475.

39. Fersht AR (1987) The hydrogen bond in molecular recognition. *Trends Biochem. Sci.* 12**:** 301-304.

40. Horovitz A, Serrano L, Avron B, Bycroft M, Fersht AR (1990) Strength and cooperativity of contributions of surface salt bridges to protein stability. *J. Mol. Biol.* 216**:** 1031-1044.

41. Rico F, Moy VT (2007) Energy landscape roughness of the streptavidin-biotin interaction. *J. Mol. Recognit.* 20**:** 495-501.

42. Janovjak H, Knaus H, Muller DJ (2007) Transmembrane helices have rough energy surfaces. *J. Am. Chem. Soc.* 129**:** 246-247.

43. Schlierf M, Rief M (2005) Temperature softening of a protein in single-molecule experiments. *J. Mol. Biol.* 354**:** 497-503.

44. Zwanzig R (1988) Diffusion in a rough potential. *Proc. Natl. Acad. Sci. USA* 85**:** 2029-2030.

45. Reed MAC et al. (2006) The denatured state under native conditions: A non-native-like collapsed state of N-PGK. *J. Mol. Biol.* 357**:** 365-372.

46. Cliff MJ et al. (2009) The denatured state of N-PGK is compact and predominantly disordered. *J. Mol. Biol.* 385**:** 266-277.

47. Redfield C (2004) Using nuclear magnetic resonance spectroscopy to study molten globule states of proteins. *Methods* 34**:** 121-132.

48. Mok KH, Nagashima T, Day IJ, Hore PJ, Dobson CM (2005) Multiple subsets of side-chain packing in partially folded states of alpha-lactalbumins. *Proc. Natl. Acad. Sci. U. S. A.* 102**:** 8899-8904.

49. Mok KH et al. (2007) A pre-existing hydrophobic collapse in the unfolded state of an ultrafast folding protein. *Nature* 447**:** 106-109.

50. Felitsky DJ, Lietzow MA, Dyson HJ, Wright PE (2008) Modeling transient collapsed states of an unfolded protein to provide insights into early folding events. *Proc. Natl. Acad. Sci. U. S. A.* 105**:** 6278-6283.

51. Schroer MA et al. (2010) High-Pressure SAXS Study of Folded and Unfolded Ensembles of Proteins. *Biophys. J.* 99**:** 3430-3437.

52. Li L, Mirny LA, Shakhnovich EI (2000) Kinetics, thermodynamics and evolution of non-native interactions in a protein folding nucleus. *Nat. Struct. Biol.* 7**:** 336-342.

53. Viguera AR, Vega C, Serrano L (2002) Unspecific hydrophobic stabilization of folding transition states. *Proc. Natl. Acad. Sci. U. S. A.* 99**:** 5349-5354.

54. Guigas G, Weiss M (2008) Sampling the cell with anomalous diffusion - The discovery of slowness. *Biophys. J.* 94**:** 90-94.

55 Baker D (2000) A surprising simplicity to protein folding. *Nature* 405**:** 39-42.

Figure Legends

Figure 1. Rugged energy landscape (schematic). (*A*) One-dimensional representation of a section of the multi-dimensional rugged potential energy landscape in conformational space, encompassing two large-scale potential energy minima (basins) corresponding to significantly different conformations and multiple local minima of varying depths, including conformations with short (solid arrows) and long (dotted arrows) trapping times. The inset schematically indicates the hierarchy of local minima with different depths on different length scales. It has to be noted that only minima with a depth of k_BT or more, where k_B is the Boltzmann constant and T the absolute temperature, will significantly affect motion over the energy landscape. Also indicated is the jump activation barrier, E, for one particular minimum. (*B*) The exponential distribution, $g(E)$, of E with a width of 3.5 k_BT which is indicated by our experimental results (solid line), in comparison with a distribution with a width of k_BT (dotted line), which would yield normal diffusion of the polypeptide backbone, both normalized to 1 at $E = 0$; the hatched area highlights the thermal energy k_BT**.** Also indicated are the trapping times associated with particular values of E, with the double-sided arrows corresponding to a range of the pre-exponential factor of 10^{11} – 10^{13} s^{-1}.

Figure 2. Schematic representation of the processes following disulfide bond photolysis of cross-linked proteins. Following cross-link photolysis, recombination to the original disulfide bond competes with backbone motions that separate the thiyl radicals and lead to folding of the protein (0-2 M urea) or to full equilibration between all unfolded conformations (8 M urea).

Figure 3. Transient thiyl radical absorbance decay after UV photolysis of cross-linked N-PGK. (*A*) Absorbance changes at 560 nm on the picosecond time scale, in the absence of urea; shown are two separate measurements, indicated by open and closed symbols, scaled to account for different experimental conditions (note the scale break indicated by the dashed line); (*B-D*) Absorbance changes at 488 nm on the nano- to millisecond time scale in the presence of 2 M and 8 M urea, respectively.

Figure 4. Time dependence of the instantaneous rate constant $k_{inst}(t)$ for thiyl radical recombination after photolysis of an aromatic disulfide cross-linker. Shown are the results for N-PGK (black), two separate measurements on the picosecond time scale in the absence of urea, indicated by open and closed symbols, and measurements on the nano- to millisecond time scale in the presence of 2 M and 8 M urea, respectively; and α-helical model peptides (22) (grey symbols). Solid lines are the results of power law fits, also given are the powers obtained from these fits.

Figure 5. Simulated time dependence of the instantaneous rate constant, $k_{inst}(t)$, for geminate recombination of thiyl radicals undergoing subdiffusive motion, for values of the subdiffusion parameter α ranging from 1 (normal diffusion) to 0.1 in steps of 0.1; model parameters: Initial pair separation r_0 = 7.2 Å, contact distance σ = 7.2 Å, diffusion constant D = 4 Å^2/ns, see Appendix III (Supplementary Information) for details and motivation of these parameters and simulations using other parameters. Highlighted are the curves for α = 1 (dashed) and α = 0.3 (bold). Inset: Power of the $k_{inst}(t)$ time dependence obtained from power law fits at short and long times, respectively, for different values of the subdiffusion parameter α.

Fig.1

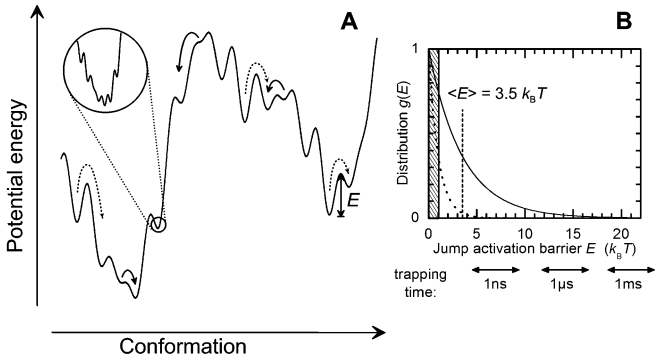
A
B
Potential energy
Conformation
E
Distribution g(E)
<E> = 3.5 $k_B T$
Jump activation barrier E ($k_B T$)
trapping time:
1ns
1µs
1ms

Fig. 2

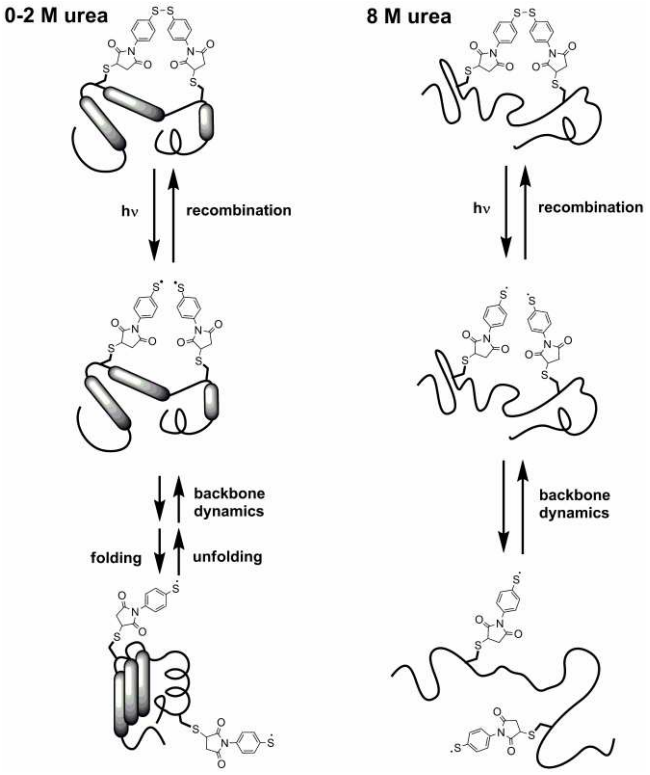
0-2 M urea
8 M urea
hν
recombination
backbone dynamics
folding
unfolding

Fig. 3

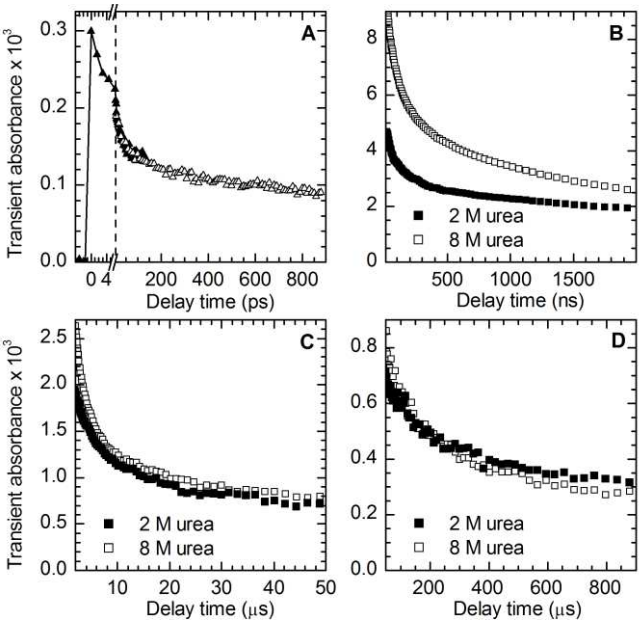

Fig. 4

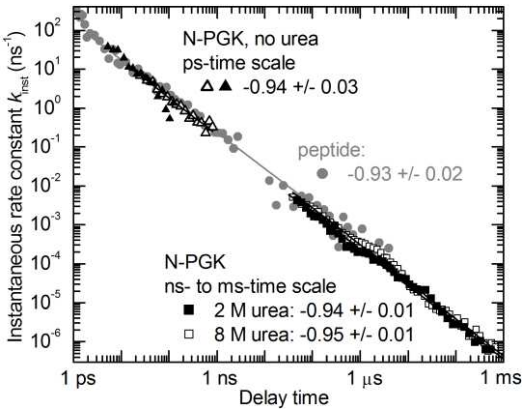

Fig. 5